Optimization of Energy Consumption for Quadrotor UAV

F. Yacef*, N. Rizoug, O. Bouhali, and M. Hamerlain
ESTACA, Laval, France
Jijel University, Jijel, Algeria
CDTA, Algiers, Algeria

ABSTRACT

In this paper we deals with the limitation of flight endurance for quadrotor unmanned aerial vehicles. Quadrotor UAVs are multi-rotors flying machines; thus, a large proportion of their energy is consumed by rotors in order to maintain the vehicle in the air. In this concept, we introduced an energetic model composed of quadrotor movement dynamic, motors dynamic and battery dynamic; then, the proposed model was validated through simulation to show possibility of saving energy. An optimal control problem is formulated and solved in order to compute minimum energy. In this problem, we seeks to find control inputs and vehicle trajectory between initial and final configurations that minimize the consumed energy during a specific mission. Simulation experiment is made for a quadrotor to highlight the proposed optimization method.

1 INTRODUCTION

In the last few years, rotary wings unmanned aerial vehicles UAVs have attract more interest due to the wide range of applications that can be addressed with such a vehicle. Recently some promising new applications have been emerged like package delivery, cinematography, agriculture surveillance and aerial manipulation; however theses applications still restricted since the embedded energy whose source is LiPo battery provide a flight time between 15 and 45 minutes, which limited the class of mission that can be carried out successfully by the UAV. To undertake this problem, many efforts have made in reduction of rotary wings UAVs weight by the use of carbon fiber airframe and high energy density intelligent-soft and in the improvement of power to weight rate. These solutions success to reduced operating in energy-starved regimes; nevertheless, no significant technological progress is made until now.

Many studies have been proposed recently contributing towards save energy and increased endurance. These contributions have mainly focused on the design of automated battery charging/replacing system. A battery swapping system for multiple small-scale UAVs have been proposed in [1]. In addition to the battery swapping mechanism, the system includes an online algorithm that can supervise replenishment of many UAVs operating simultaneously, determine when the vehicle require replenishment and perform a precision landing onto the battery swapping mechanism's landing platform. In [2] the design, test and construction of an autonomous ground recharge station for battery-powered quadrotor helicopter was presented. An energy management algorithm was implemented for a multi-agent system where the priority is given to the group to ensure the optimality of the solution regardless of number, position and density of the environment. Where in [3], an autonomous battery maintenance mechatronic system to extends the operational time of battery powered small-scaled UAVs have been developed.

Other studies have introduce endurance estimation model, in [4] a simple model is proposed to estimate the endurance of an indoor hovering quadrotor, whereas in [5] a characterization of the power consumption of rotorcraft supplied by LiPo battery and an accurate endurance estimation model have been introduced. In order to extends UAVs operating time a battery state of charge based altitude controller for an six-rotor aircraft was proposed in [6], where a battery monitoring system was designed in order to estimate state of charge (SOC) and then use it to calculate the designed controller.

In view of path following control with minimum energy consumption, the authors in [7] evaluate the relationship between navigation speed and energy consumption in a miniature quadrotor helicopter, which travels over a desired path through experimental test. Then, a novel path-following controller is proposed in which the speed of the rotorcraft is a dynamic profile that varies with the geometric requirements of the desired path.

The energy optimal path planning problem for rotary wings UAVs has gain less interest in the unmanned aerial systems literature. In [8] an approach has been proposed to solve near-minimum-energy tours for an hexarotor on a multi-target mission using the generalized traveling salesman problem with Neighborhoods and a heuristic algorithm with 4-DOF dynamic model for cost function calculation. Where in [9] minimum-energy paths were obtained between given initial and final configurations for a 6-DOF quadrotor UAV by solving an optimal control problem, also a minimum-time and/or minimum-control-effort trajectory was calculated by

*Email : fyacef@cdta.dz, fouad.yacef@estaca.fr

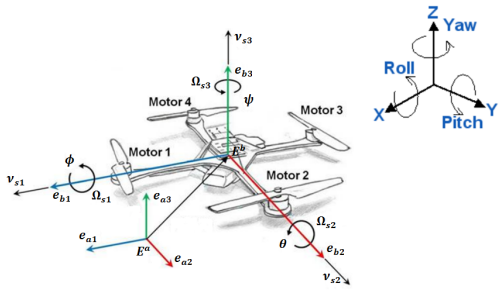

Figure 1: Quadrotor scheme

solving a related optimal control problem.

Motivated by the previous discussion, in this paper we introduced an energetic model for quadrotor UAVs. The proposed energetic model contains the vehicle dynamic, actuator dynamic and battery dynamic with an efficiency function in order to modeled motor efficiency and have an energetic model close to reality. Then, we proposed an energy optimal control problem, where the objective is to minimize the energy consumed by the quadrotor vehicle at the end of the mission while the quadrotor aircraft has to satisfy boundary conditions and feasibility constraints on the states of the system and control inputs.

The rest of this paper is organized as follows. In section 2, we presented Energetic model. Then, in section 3 Energy optimization problem is introduced. In section 4, nonlinear programming method and simulation results are presented. Conclusions and remarks are drawn in section 5.

2 Energetic model

Before proceeded in energy optimization we need an energetic model in order to have an idea about the energy consumed by the vehicle during the mission and provide a direct relation between energy and vehicle dynamic's.

2.1 Quadrotor dynamic model

In this section, we will first introduce the quadrotor unmanned aerial flying vehicles coordinate system as depicted in Fig. 1. To study the system motion dynamics, two frames are used: an inertial frame attached to the earth defined by $E^a(e_{a1}, e_{a2}, e_{a3})$ and a body-fixed frame $E^b(e_{b1}, e_{b2}, e_{b3})$ fixed to the center of mass of the quadrotor. The absolute position of the quadrotor is described by $p = [x, y, z]^T$ and its attitude by the Euler angles $\eta = [\phi, \theta, \psi]^T$. The attitude angles are respectively Yaw angle (ψ rotation around z-axis), Pitch angle ((θ rotation around y-axis), and roll angle (ϕ rotation around x-axis) [10]. The dynamic model for quadrotor vehicle can be derived as

$$\begin{aligned} m\ddot{x} &= (\cos\phi\sin\theta\cos\psi + \sin\phi\sin\psi)T \\ m\ddot{y} &= (\cos\phi\sin\theta\sin\psi - \sin\phi\cos\psi)T \\ m\ddot{z} &= (\cos\phi\cos\theta)T - mg \\ I_x\ddot{\phi} &= (I_y - I_z)\dot{\theta}\dot{\psi} + J\dot{\theta}\varpi + lu_1 \\ I_y\ddot{\theta} &= (I_z - I_x)\dot{\phi}\dot{\psi} - J\dot{\phi}\varpi + lu_2 \\ I_z\ddot{\psi} &= (I_x - I_y)\dot{\phi}\dot{\theta} + u_3 \end{aligned} \tag{1}$$

where $\varpi = \omega_1 - \omega_2 + \omega_3 - \omega_4$. where J is the rotor inertia, m, I_x, I_y and I_z denotes the mass of the quadrotor flying vehicle and inertia, l is the distance from the center of mass to the rotor shaft, κ_b is the thrust factor and ω_j $j = 1, \ldots, 4$ is the motor speed, $g = 9.81m/s^2$ is the acceleration due to gravity.

The control inputs are given as follows:

$$\begin{cases} T = \kappa_b(\omega_1^2 + \omega_2^2 + \omega_3^2 + \omega_4^2) \\ u_1 = \kappa_b(\omega_2^2 - \omega_4^2) \\ u_2 = \kappa_b(\omega_3^2 - \omega_1^2) \\ u_3 = \kappa_\tau(\omega_1^2 - \omega_2^2 + \omega_3^2 - \omega_4^2) \end{cases}$$

Remark 1. The Euler angles roll and pitch are assumed to be limited to $-\pi/2 < \phi < \pi/2$, $-\pi/2 < \theta < \pi/2$. This assumption is common in practice since the quadrotor vehicle does not perform aggressive maneuvers over free flight.

2.2 Actuator dynamic

A quadrotor UAV actuator system is typically consist of a LiPo battery, a brushless direct current (BLDC) motor and an control stage to control the angular velocity (RPM) of the motor. Electrical DC motors are well modeled by a circuit containing a resistor, inductor, and voltage generator in series [11].

$$v(t) = Ri(t) + L\frac{\partial i(t)}{\partial t} + \frac{\omega(t)}{k_v} \tag{2}$$

where R is the motor internal resistance, L is the inductance, $\omega(t)$ is the rotational rat of the motor, and k_v is the voltage constant of the motor, expressed in $rad/s/volt$. Also, the motor torque τ can be modeled as being proportional to the current $i(t)$ through the torque constant, k_t, expressed in Nm/A.

$$\tau(t) = k_t i(t) \tag{3}$$

The motor dynamics are modeled as a simple first order differential equation (4) where $\dot{\omega}$ is driven by the motor torque and the load friction torque $Q_f(\omega(t))$. The inertia, J includes the motor and the propeller, the motor torque comes from the voltage generator, and the load friction torque results from the propeller drag $Q_f(\omega(t)) = \kappa_\tau\omega^2(t)$, κ_τ is the drag coefficient.

$$J\frac{\partial\omega(t)}{\partial t} = \tau(t) - Q_f(\omega(t)) - D_v\omega(t) \tag{4}$$

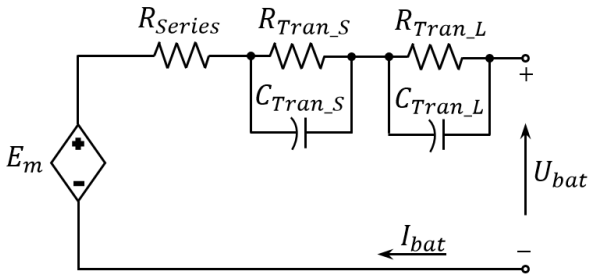

Figure 2: Battery scheme

where D_v is the viscous damping coefficient of the motor Nms/rad. Typically, the inductance of small, DC motors is neglected compared to the physical response of the system and so can be ignored. Under steady-state conditions, the current $i(t)$ is constant, and equation (2) reduces to :

$$v(t) = Ri(t) + \frac{\omega(t)}{k_v} \tag{5}$$

where the term $\frac{1}{k_v}\omega(t)$ represent the electromotive force of the motor. Table 1 shows the motor coefficients for the BLDC motor used in our study.

Parameter	Value
$J\ (kg.m^2)$	$4.1904e^{-5}$
$k_t\ (N.m/A)$	$0.0104e^{-3}$
$k_v\ (rad/s/volt)$	96.342
$D_v(Nms/rad)$	$0.2e^{-3}$
$R\ (Ohm)$	0.2

Table 1: Motor Coefficients

2.3 Battery dynamic

Li-ion battery possesses the greatest potential for future development and optimization. In addition to small size and low weight the Li-ion batteries offer the highest energy density and storage efficiency close to 100%, which makes them ideally suited for portable devices. But the major drawbacks of this type are its high cost [12] [13].

A physical Li-ion battery model was presented. The battery model was designed to accept inputs for current. The outputs were voltage and state of charge (SOC). This model does not take into account the influence of temperature and the phenomenon of self-discharge [12]. However, it gives results close to reality. The model is based on the two equations, the state of charge (SOC) and The voltage across the cell.

$$SOC = 100\left[1 - \frac{\int I}{Q}\right] \tag{6}$$

$$U_{bat} = E_m - R_{int}I \tag{7}$$

E_m is the open circuit voltage (VOC). Its expression is as follows:

$$E_m = E_0 - K\left[\frac{Q}{Q - \int I}\right] + Ae^{-B\int I} \tag{8}$$

E_0 is the open circuit voltage at full load, this is different from the nominal voltage given by the manufacturers. Q is the cell capacity in Ah, The parameters K bias voltage, A exponential voltage and B exponential capacity are experimental parameters determined from discharge curve.

Parameter	Value
$Q\ (Ah)$	1.55
$R_{int}\ (Ohm)$	0.02
$E_0\ (volt)$	1.24
$K\ (volt)$	$2.92e^{-3}$
A	0.156
B	2.35

Table 2: Battery parameters

The model is nonlinear, it was necessary to adapt the input current to that seen by an elementary cell by dividing to parallel branch number $M_{bat} = 1$. For output voltage of our battery, we simply multiplied the output voltage of the cell by the series branch number $N_{bat} = 3$. This methodology requires hypothesize that the cells have the same behavior.

2.4 Energy and motor efficiency

Firsts let define the energy consumed by the vehicle during the mission.

$$E_c = \int_{t_0}^{t_f} \sum_{j=1}^{4} \tau_j(t)\omega_j(t)dt \tag{9}$$

with $\tau_j(t)$ is the torque generated by motor j and $\omega_j(t)$ is rotor speed at time t. By using equation (4) for the four motors, equation (9) can be rewrite as follow:

$$E_c = \int_{t_0}^{t_f} \sum_{j=1}^{4} \Big(J\dot{\omega}_j(t) + \kappa_\tau\omega_j^2(t) + D_v\omega_j(t)\Big)\omega_j(t)dt \tag{10}$$

In order to make our energetic model more realistic, an efficiency function is identified and added to energy function (9). The efficiency of the brushless dc motor used for actuate quadrotor helicopter is function of motor torque and rotor speed $f_r(\tau(t), \omega(t))$. We have used polynomial interpolation for efficiency function identification, thus $f_r(\tau(t), \omega(t))$ can be formulated as follow:

$$\begin{aligned} f_r\big(\tau(t), \omega(t)\big) = a\big(\omega(t)\big)\tau^3(t) + b\big(\omega(t)\big)\tau^2(t) \\ + c\big(\omega(t)\big)\tau(t) + d\big(\omega(t)\big) \end{aligned} \tag{11}$$

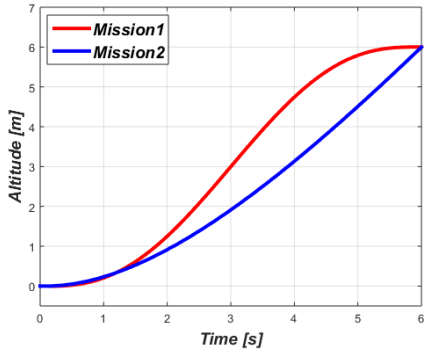

(a)

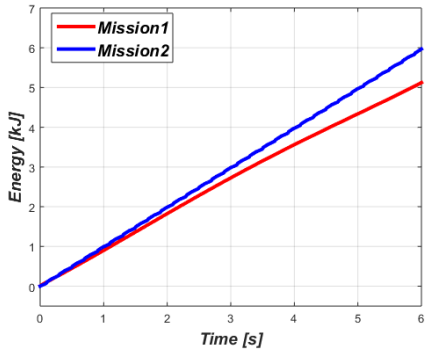

(b)

Figure 3: Quadrotor altitude (a) and consumed energy (b)

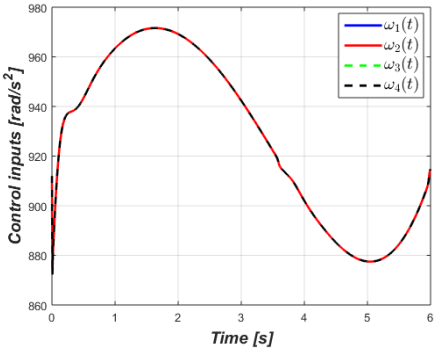

(a)

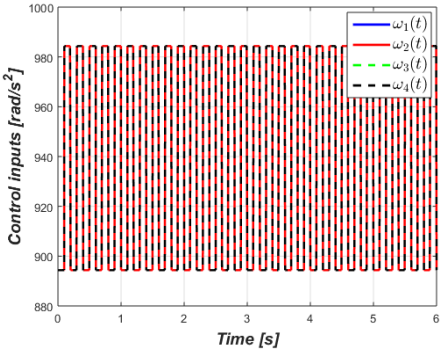

(b)

Figure 4: Control inputs, mission1 (a) mission2 (b)

and

$$a(\omega(t)) = a_1\omega^2(t) + b_1\omega(t) + c_1$$
$$b(\omega(t)) = a_2\omega^2(t) + b_2\omega(t) + c_2$$
$$c(\omega(t)) = a_3\omega^2(t) + b_3\omega(t) + c_3$$
$$d(\omega(t)) = a_4\omega^2(t) + b_4\omega(t) + c_4$$

The parameters of the polynomial are calculated using Matlab for the four motors (we assume that the motors are identical).

$$a_1 = -1.72\ 10^{-5} \qquad b_1 = 0.014 \qquad c_1 = -0.8796$$
$$a_2 = 1.95\ 10^{-5} \qquad b_2 = -0.0157 \qquad c_2 = 0.3385$$
$$a_3 = -6.98\ 10^{-6} \qquad b_3 = 5.656\ 10^{-3} \qquad c_3 = 0.2890$$
$$a_4 = 4.09\ 10^{-7} \qquad b_4 = -3.908\ 10^{-4} \qquad c_4 = 0.1626$$

Then the consumed energy (10) can be rewrite as

$$E_c = \int_{t_0}^{t_f} \sum_{j=1}^{4} \frac{\left(J\dot{\omega}_j(t) + \kappa_\tau\omega_j^2(t) + D_v\omega_j(t)\right)}{f_{r,j}\left(\tau_j(t), \omega_j(t)\right)}\omega_j(t)dt \tag{12}$$

2.5 *Effect of control inputs on energy consumption*

In order to validate the proposed energetic model, we have simulated tow vertical take-off mission with two different altitude trajectory as depicted in Fig. 3-a, and different control inputs as shown in Fig. 4. The missions have the same duration $t_f = 6s$ and the same initial and final configuration.

We have calculate the consumed energy for two mission using equation (12). For the first mission (red line) the consumed energy is $E_1 = 5.12kJ$, where in second mission (blue line) the consumed energy is $E_2 = 5.97kJ$; thus the gain between two mission with the same initial and final configuration is 17%. For a specific mission, energy optimization ca be achieved; what we need is to find control inputs and trajectory that give optimal consumption of energy.

3 Energy Optimization

The energy optimization problem seeks to find control inputs and trajectory for quadrotor helicopter that minimize the consumed energy while satisfying a set of constraints on states and control inputs. In view of optimal control, we try to compute an open-loop solution to an optimal control problem. We looking for control inputs of system (1) that minimize the

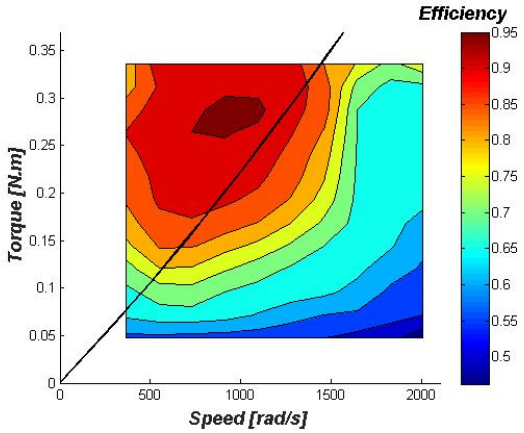

Figure 5: Brushless motor efficiency

consumed energy during a mission between two specific initial and final configurations.

3.1 Problem statement

Now the problem of optimal energy trajectory planning can be formulated as a minimization problem, by which the final consumed energy $E_c(tf)$ is used as the cost function. In addition the state variables in $[x, \dot{x}, y, \dot{y}, z, \dot{z}, \phi, \dot{\phi}, \theta, \dot{\theta}, \psi, \dot{\psi}]^T$ and control variables in $[\omega_1, \omega_2, \omega_3, \omega_4]^T$ are constrained to satisfy the vehicle dynamics (1) and boundary conditions. The mission is to fly between specified initial and final positions during a time interval $[t_0, t_f]$ where t_0 and t_f are given.

Based on the above description, the optimal control problem can be formulated as:

$$\min_{(\omega_j, \tau_j)} E_c(t_f) \tag{13}$$

subject to

$$\begin{aligned} m\ddot{x} &= (\cos\phi \sin\theta \cos\psi + \sin\phi \sin\psi)T \\ m\ddot{y} &= (\cos\phi \sin\theta \sin\psi - \sin\phi \cos\psi)T \\ m\ddot{z} &= (\cos\phi \cos\theta)T - mg \\ I_x\ddot{\phi} &= (I_y - I_z)\dot{\theta}\dot{\psi} + J\dot{\theta}\varpi + lu_1 \\ I_y\ddot{\theta} &= (I_z - I_x)\dot{\phi}\dot{\psi} - J\dot{\phi}\varpi + lu_2 \\ I_z\ddot{\psi} &= (I_x - I_y)\dot{\phi}\dot{\theta} + u_3 \end{aligned} \tag{14}$$

and

$$\begin{aligned} |\phi| \leq \frac{\pi}{2},\ |\theta| \leq \frac{\pi}{2},\ |\dot{\psi}| \leq \dot{\Psi} \\ \omega_{min} \leq \omega_j \leq \omega_{max} \\ 0 \leq T \leq T_{max},\ |u_k| \leq u_{max},\ k = 1, 2, 3 \end{aligned} \tag{15}$$

with boundary conditions:

$$\begin{aligned} [x(t_0), y(t_0), z(t_0), \phi(t_0), \theta(t_0), \psi(t_0)]^T = \\ [x_0, y_0, z_0, \phi_0, \theta_0, \psi_0]^T \\ [x(t_f), y(t_f), z(t_f)]^T = [x_f, y_f, z_f]^T \end{aligned} \tag{16}$$

The additional constraints in (16) are associated with vehicle dynamics where ω_{min} and ω_{max} are the minimum and maximum feasible velocity of the aircraft rotors, respectively. The roll and pitch angles, $\phi,\ \theta$, have to satisfy $|\phi| \leq \frac{\pi}{2},\ |\theta| \leq \frac{\pi}{2}$ based on their physical definition, and $|\dot{\psi}| \leq \dot{\Psi}$ is required to generate a smooth trajectory where $\dot{\Psi}$ is the maximum changing rate of the heading angle.

4 Nonlinear programming and simulation results

4.1 Nonlinear programming method

The optimal control problem presented in the previous sections (13)-(17) is a complex nonlinear optimization problem. The general approach to solve this problem is the direct collocation method. The basic idea of direct collocation is to discretize a continuous solution to a problem represented by state and control variables by using linear interpolation to satisfy the differential equations. In this way an optimal control problem is transformed into a nonlinear programming problem (NLPP).

In our study, the proposed optimal control problem have been numerically solved using a Matlab software called GPOPS-II [14]. The software employs a Legendre-Gauss-Radau (LGR) [15][16] quadrature orthogonal collocation method where the continuous-time optimal control problem is transcribed to a large sparse nonlinear programming problem (NLP). it used an adaptive mesh refinement method that determines the number of mesh intervals and the degree of the approximating polynomial within each mesh interval to achieve a specified accuracy. The software allows the use of two nonlinear programming (NLP) solver used to solve the NLPP. The first is the open-source NLP solver IPOPT (Interior Point OPTimizer) [17], where the second is the NLP solver SNOPT (Sparse Nonlinear OPTimizer) [18].

4.2 Simulation Results

Problem (13)-(17) was solved using the open-source NLP solver IPOPT in second derivative (full Newton) mode with the publicly available multi-frontal massively parallel sparse direct linear solver MUMPS [19]. All results were obtained using the implicit integration form of the Radau collocation method and various forms of the aforementioned *ph* mesh refinement method using default NLP solver settings and the automatic scaling routine in GPOPS-II.

In our tests we considered the DJI Phantom 2 quadrotor [20] with multi-rotor propulsion system (2212/920KV motors). The physical parameters of the Phantom 2 used in the simulation experiment, are reported in Table 3.

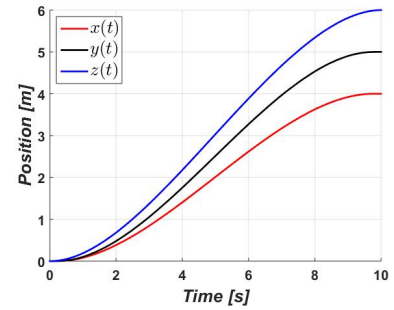

(a)

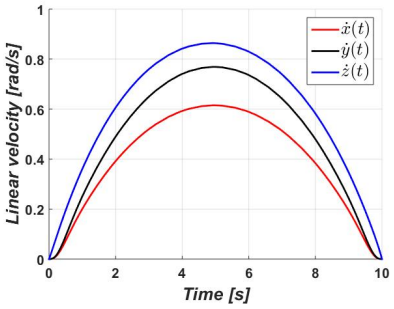

(b)

Figure 6: Quadrotor position (a) and linear velocity during the trajectory (b)

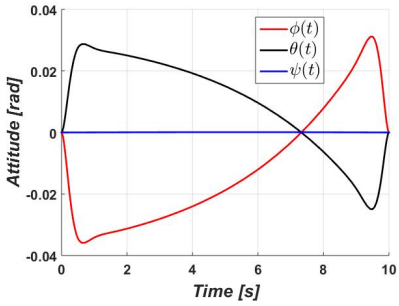

(a)

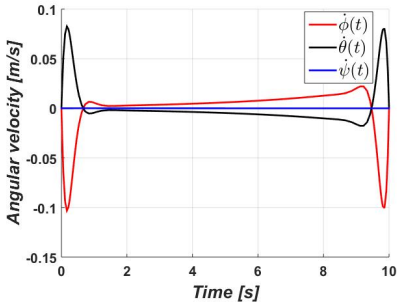

(b)

Figure 7: Quadrotor attitude (a) and angular velocity (b)

The problem (13)-(17) was numerically solved to find the minimum energy control inputs $\omega_j(t)$ that allows quadrotor to fly from the initial position $[x, y, z]^T = [0, 0, 0]^T$ at time $t_0 = 0$ to the final one $[x, y, z]^T = [4, 5, 6]^T$ at time $t_f = 10s$, with initial condition $[x_0, y_0, z_0, \phi_0, \theta_0, \psi_0]^T = [0_{1\times6}]^T$ and final condition $[x_f, y_f, z_f, \phi_f, \theta_f, \psi_f]^T = [4, 5, 6, 0, 0, 0]^T$. Null initial angular and linear velocities were considered $[\dot{x}_0, \dot{y}_0, \dot{z}_0, \dot{\phi}_0, \dot{\theta}_0, \dot{\psi}_0]^T = [0_{1\times6}]^T$ and the same for final angular and linear velocities . With respect to constraints in (12) the initial guess for inputs control is given by $w_s = 912,32\ rad/s$ which means that the total thrust is $T = 12,75\ N$ which corresponds the thrust necessary to counterbalance the gravity acceleration. Fig. 6 shows the time evolutions of the vehicle position and linear velocity, were Fig. 7 shows the time evolutions of the vehicle attitude and angular velocity. Fig. 8 reports The optimal trajectory in $(x - y - z)$ space and the control inputs $\omega_j(t)$. The energy consumed by the quadrotor to ravel this trajectory is $E_c(t_f) = 10.38\ kJ$ Fig. 9.

4.3 Comparative study

In order to evaluate the energy consumed by the vehicle and have an idea about the saving energy with the proposed approach, we have compared the energy consumed by the quadrotor vehicle under our optimal control approach and the energy consumed under a classical control approach.

The classical control approach consist of two controller, a low-level controller and the high-level control algorithm for quadrotor vehicle.

The low-level control module consist of an adaptive fuzzy backstepping controller [10], composed of three terms , the fuzzy adaptive control term which is designed to approximate a model-based backstepping control law $u_{f,j} = \Theta_j^T \varphi_j(x_s)$, where Θ_j^T is the vector of fuzzy basis functions, $\varphi_j(x_s)$ is the vector of adjustable parameters of the fuzzy logic system and x_s is the state vector. The bounded robust control term $u_{r,j} = \hat{\delta}_j \tanh(\frac{e_{2j}}{\epsilon_j})$ employed to compensate the fuzzy approximation error. Finally, $u_{p,j} = k_{2j} e_{2j}$ the proportional derivative term.

The tracking errors is defined as:

$$e_{1j} = x_{1j,d} - x_{1j}\ ,\ j = 1, \ldots, 6 \tag{17}$$

where $x_{1j,d}$ is the position and attitude desired signals. Using position controller u_5 and u_6 (18), the desired roll and pitch signals can be calculated as $\theta_d = atan(\frac{u_5 \cos\psi + u_6 \sin\psi}{g})$, $\phi_d = atan(\frac{u_5 \sin\psi - u_6 \cos\psi}{g} \cos\theta_d)$. The backstepping second tracking errors signals is defined as

$$e_{2j} = \upsilon_j - x_{2j} \tag{18}$$

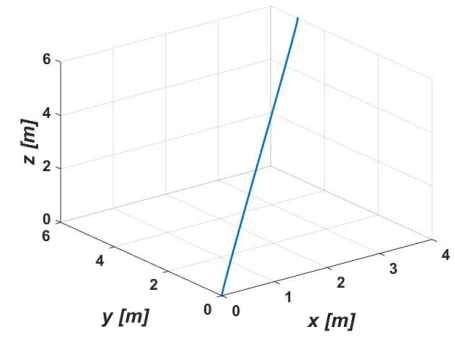

(a)

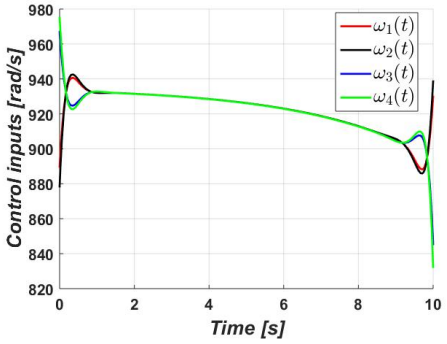

(b)

Figure 8: The optimal trajectory in $(x-y-z)$ space (a), and the control inputs (b)

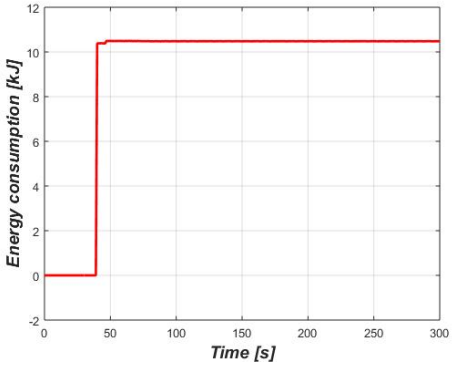

Figure 9: Cost function $E_c(t)$

with the virtual control law $\upsilon_i = \dot{x}_{1j,d} + k_{1j}e_{1j}$ and $k_{1j} > 0$. Then, we introduce the following tracking control algorithm.

$$u_j(t) = \Theta_j^T \varphi_j(x_s) + \hat{\delta}_j \tanh\left(\frac{e_{2j}}{\epsilon_j}\right) + k_{2j}e_{2j} \qquad (19)$$

$$\dot{\Theta}_j = \gamma_j e_{2i} \varphi_j(x_s) \qquad (20)$$

$$\dot{\hat{\delta}}_j = \eta_j e_{2j} \tanh\left(\frac{e_{2j}}{\epsilon_j}\right) \qquad (21)$$

where $k_{2j} > 0, \epsilon_j > 0, \gamma_j > 0, \eta_j > 0$ are design parameters.

The high-level control algorithm consist of a third degree polynomial, $q(t) = \alpha_0 + \alpha_1 t + \alpha_2 t^2 + \alpha_3 t^3$, with initial and final conditions on position and velocity $q(t_0) = q_0,\ q(t_f) = q_f,\ \dot{q}(t_0) = \dot{q}_0,\ \dot{q}(t_f) = \dot{q}_f$ we can calculate parameters of the polynomial.

4.4 Comparison

The consumed energy obtained with the classical approach is $E_c(t_f) = 10.49\ kJ$, compared to the energy consumed by the proposed approach, its increase with 1% from the total energy, which is not a good saving quantity of energy. To improve the saving quantity of energy we must make he model more energetic, which will be the objective of future work.

We have made a comparative study between our approach and the approach proposed by [9] for a final time $t_f = 20s$. The consumed energy obtained with the approach proposed in [9] is $E_{c1}(t_f) = 26.23\ kJ$, where the energy consumed by our approach for the same boundary conditions is $E_{c2}(t_f) = 20.72\ kJ$. The energy saved by the proposed approach compared to the one proposed in [9] is 26.59% from the total energy.

Parameter	Value
$l\ (m)$	0.175
$m\ (kg)$	1.3
$I_x\ (kgm^2)$	0.081
$I_y\ (kgm^2)$	0.081
$I_z\ (kgm^2)$	0.142
$\kappa_b\ (N/rad/s)$	$3.8305e^{-6}$
$\kappa_\tau\ (Nm/rad/s)$	$2.2518e^{-8}$

Table 3: Quadrotor parameters

5 Conclusion and Future Work

In this paper we have introduced an energetic model for quadrotor vehicle. The energetic model contains vehicle movement dynamic, actuators dynamic, battery dynamic and an efficiency function for energy computing. Then, we have validated the energetic model through two different mission with the same initial and final configurations. For energy optimization purpose, an optimal control problem have been introduced and solved using an optimal control software GPOPS-II. In the optimal control problem we seeks to find the vehicle control inputs and trajectory that minimize the consumed energy during a specific mission. The numerical experiments illustrated the solutions of the proposed optimal control problem, and the comparative study provide quantization of energy that can be saved in a simple mission.

In future work, we will incorporate propeller aerodynamic to improve the energetic model, and we will introduce an energy optimization problem with respect to battery life. We are also going to advise an experimental procedure to validate the proposed approach.

REFERENCES

[1] Kurt A Swieringa, Clarence B Hanson, Johnhenri R Richardson, Jonathan D White, Zahid Hasan, Elizabeth Qian, and Anouck Girard. Autonomous battery swapping system for small-scale helicopters. In *Robotics and Automation (ICRA), IEEE International Conference on*, pages 3335–3340, 2010.

[2] Jeremie Leonard, Al Savvaris, and Antonios Tsourdos. Energy management in swarm of unmanned aerial vehicles. *Journal of Intelligent & Robotic Systems*, 74(1-2):233–250, 2014.

[3] N Kemal Ure, Girish Chowdhary, Tuna Toksoz, Jonathan P How, Matthew A Vavrina, and John Vian. An automated battery management system to enable persistent missions with multiple aerial vehicles. *Mechatronics, IEEE/ASME Transactions on*, 20(1):275–286, 2015.

[4] James F Roberts, Jean-Christophe Zufferey, and Dario Floreano. Energy management for indoor hovering robots. In *Intelligent Robots and Systems (IROS), IEEE/RSJ International Conference on*, pages 1242–1247, 2008.

[5] Analiza Abdilla, Arthur Richards, and Stephen Burrow. Power and endurance modelling of battery-powered rotorcraft. In *Intelligent Robots and Systems (IROS), 2015 IEEE/RSJ International Conference on*, pages 675–680, 2015.

[6] Michal Podhradskỳ, Calvin Coopmans, and Austin Jensen. Battery state-of-charge based altitude controller for small, low cost multirotor unmanned aerial vehicles. *Journal of Intelligent & Robotic Systems*, 74(1-2):193–207, 2014.

[7] D. C. Gandolfo, L. R. Salinas, A. Brando, and J. M. Toibero. Stable path-following control for a quadrotor helicopter considering energy consumption. *IEEE Transactions on Control Systems Technology*, PP(99):1–8, 2016.

[8] Kevin Vicencio, Tristan Korras, Kenneth A Bordignon, and Iacopo Gentilini. Energy-optimal path planning for six-rotors on multi-target missions. In *Intelligent Robots and Systems (IROS), 2015 IEEE/RSJ International Conference on*, pages 2481–2487, 2015.

[9] Fabio Morbidi, Roel Cano, and David Lara. Minimum-energy path generation for a quadrotor uav. In *Robotics and Automation (ICRA), IEEE International Conference on*, 2016.

[10] Fouad Yacef, Omar Bouhali, Mustapha Hamerlain, and Nassim Rizoug. Observer-based adaptive fuzzy backstepping tracking control of quadrotor unmanned aerial vehicle powered by li-ion battery. *Journal of Intelligent & Robotic Systems*, 84(1):179–197, 2016.

[11] Mark Cutler, N Kemal Ure, Bernard Michini, and Jonathan P How. Comparison of fixed and variable pitch actuators for agile quadrotors. In *AIAA Conference on Guidance, Navigation and Control*, 2011.

[12] Tedjani Mesbahi, Nassim Rizoug, Patrick Bartholomeus, and Philippe Le Moigne. Li-ion battery emulator for electric vehicle applications. In *2013 IEEE Vehicle Power and Propulsion Conference (VPPC)*, pages 1–8. IEEE, 2013.

[13] KC Divya and Jacob Østergaard. Battery energy storage technology for power systemsan overview. *Electric Power Systems Research*, 79(4):511–520, 2009.

[14] Michael A. Patterson and Anil V. Rao. Gpops-ii: A matlab software for solving multiple-phase optimal control problems using hp-adaptive gaussian quadrature collocation methods and sparse nonlinear programming. *ACM Trans. Math. Softw.*, 41(1):1:1–1:37, October 2014.

[15] Divya Garg, William W. Hager, and Anil V. Rao. Pseudospectral methods for solving infinite-horizon optimal control problems. *Automatica*, 47(4):829 – 837, 2011.

[16] Michael A Patterson and Anil Rao. Exploiting sparsity in direct collocation pseudospectral methods for solving optimal control problems. *Journal of Spacecraft and Rockets*, 49(2):354–377, 2012.

[17] Lorenz T Biegler, Omar Ghattas, Matthias Heinkenschloss, and Bart van Bloemen Waanders. Large-scale pde-constrained optimization: an introduction. In *Large-Scale PDE-Constrained Optimization*, pages 3–13. Springer, 2003.

[18] Philip E Gill, Walter Murray, and Michael A Saunders. Snopt: An sqp algorithm for large-scale constrained optimization. *SIAM review*, 47(1):99–131, 2005.

[19] P. R. Amestoy, I. S. Duff, J. Koster, and J.-Y. L'Excellent. A fully asynchronous multifrontal solver using distributed dynamic scheduling. *SIAM Journal on Matrix Analysis and Applications*, 23(1):15–41, 2001.

[20] DJI Phantom 2. http://www.dji.com/fr/phantom-2. Accessed: 2016-02-25.